SPMSM Adaptive Control With Guaranteed Dynamic Response Under Parameter Mismatch

Jiong Li, Yao Sun, *Member, IEEE*, Hanbing Dan, *Senior Member, IEEE*, Xing Li, Feng Zhou, *Member, IEEE*, and Mei Su, *Member, IEEE*

***Abstract*—The dynamic performance of the surface-mounted permanent magnet synchronous motors (SPMSM) will be affected by the moment of inertia mismatch. To guarantee the desired dynamic response of the motors under parameter mismatch, we propose an adaptive speed controller characterized by the invariable closed-loop pole. Due to the adaptive laws in the speed controller being designed to satisfy the persistent excitation condition, the closed-loop poles of the SPMSM control system do not change with the parameter drift. In addition, an adaptive current controller is designed following the immersion and invariance technique, which is able to guarantee that the estimation error of the stator resistance and magnet flux linkage are globally convergent. Finally, the proposed control scheme is verified by simulation and experimental results.**

***Index Terms*—Adaptive control, cascade control, model reference adaptive control (MRAC), surface-mounted permanent magnet synchronous motor (SPMSM).**

I. Introduction

With its high efficiency, high power density, and precise control capabilities, permanent magnet synchronous motors (PMSM) have been widely used in industrial manufacturing fields, such as electric vehicles, elevators, numerical control machine tools, and so on [1], [2], [3]. However, the PMSM system is a nonlinear system with many parameter uncertainties and unknown perturbations [4], which brings great challenges to the controller design.

In order to overcome the abovementioned challenges, many control schemes for PMSM have been deeply studied, such as direct torque control (DTC) and field-oriented control (FOC). Compared with DTC, the FOC is widely used in PMSM systems due to its lower current harmonic and torque ripple [5]. The dual loop PI controller with a cascaded control structure is one of the most common controllers in FOC control, which is simple in design and easy to implement [6]. However, the conventional PI controller is sensitive to the uncertainty of the system, which means the satisfactory control performance cannot be obtained under a wide range of parameter uncertainties and load disturbances.

To achieve faster dynamic response and robustness against parameter uncertainties, many nonlinear control schemes have been proposed for PMSM systems. The sliding mode control has been widely used because it could theoretically ensure robustness under specific premises [7], [8], [9]. Robustness is obtained, but discontinuous control laws bring unnecessary chatting to the system, which reduces the control performance of the system. The high-order sliding mode control schemes for PMSM control systems have been designed in [10] and [11] to reduce chattering. However, the robustness of the controller is guaranteed by the upper and lower bounds of the parameters, which leads to the conservative design of the system and unnecessary performance loss. Combining the disturbance observer (DOB) with other control schemes is another option for PMSM speed controllers [12], [13], [14]. As the disturbance includes the state of the system, there is no guarantee that the estimation error of the DOB will always converge to zero. Fuzzy logic control considers the uncertainty of system parameters, and with the increase in the number of fuzzy rules, the control performance will become better and better [15], [16], [17]. However, the scheme requires a lot of online computational, which brings a heavy computational burden to the controller.

In addition, adaptive control is one of the most effective methods to solve parameter uncertainty and external disturbances. Several adaptive controllers were proposed for different design objectives, such as adaptive fuzzy control [18], [19], adaptive compensation feedback control [20], [21], [22], adaptive backstepping control [23], [24], [25], and model reference adaptive control (MRAC) [26], [27], [28], [29], [30]. The adaptive speed controller proposed in [21] considers parametric uncertainties. However, the controller requires the information of acceleration speed, which is difficult to obtain. Li and Liu [22] combined adaptive control with an extended state observer to solve the problem of disturbance uncertainty. A backstepping adaptive control is proposed in [23], but the controller requires true values of inductance and flux. Using a coordinate transformation, Kim

Received 1 April 2024; revised 18 June 2024; accepted 18 August 2024. Date of publication 20 August 2024; date of current version 7 October 2024. This work was supported in part by the National Natural Science Foundation of China under Grant 62125308, Grant 52337008, Grant 52377183, and Grant 52377168 and in part by the Provincial Natural Science Foundation of Hunan under Grant 2022JJ30141. Recommended for publication by Associate Editor M. Hartmann. *(Corresponding authors: Yao Sun; Feng Zhou.)*

Jiong Li, Yao Sun, Hanbing Dan, and Mei Su are with the School of Automation, Central South University, Changsha 410083, China, and also with the Hunan Provincial Key Laboratory of Power Electronics Equipment and Grid, Changsha 410083, China (e-mail: 224601002@csu.edu.cn; yaosun@mail.csu.edu.cn; hanbingdan@csu.edu.cn; sumeicsu@csu.edu.cn).

Xing Li is with the College of Electrical and Information Engineering, Hunan University, Changsha 410082, China (e-mail: lxhnu@hnu.edu.cn).

Feng Zhou is with the College of Electronic Information and Electrical Engineering, Changsha University, Changsha 410082, China (e-mail: zhoufeng@ccsu.edu.cn).

Color versions of one or more figures in this article are available at https://doi.org/10.1109/TPEL.2024.3446816.

Digital Object Identifier 10.1109/TPEL.2024.3446816

et al. [24] proposed an adaptive control that does not require the information of parameters. However, the steady-state error of the speed is only guaranteed to be bounded and the convergence is not obtained. An integral type MRAC speed controller is proposed in [26] to solve the problem of uncertain parameters, which consists of an adaptive compensating control term and a stabilizing feedback control term. It can be found that there are some feasible methods for the control problem of parameter uncertainty in PMSMs, but the abovementioned methods cannot guarantee the adaptive terms converge to the true values, which means the dynamic performance will deteriorate with the parameter variations.

This article proposes a cascaded adaptive control scheme for a surface-mounted permanent magnet synchronous motor (SPMSM) drive, which has the following advantages.

1) The proposed adaptive speed controller characterized by the invariable closed-loop pole can guarantee the desired dynamic response of the motors under parameter mismatch.
2) The stator resistance and the rotor flux linkage are estimated based on the immersion and invariance (I&I) methodology, which can be used to provide overheating protection and demagnetization protection.

The rest of this article is organized as follows. The model of the SPMSM system and the control objectives are introduced in Section II. In Section III, the cascaded adaptive control scheme and the updated laws of adaptive terms are derived based on the Lyapunov approach. Furthermore, the existence of persistent excitation (PE) condition and the stability of the controller are proved, respectively. Section IV presents the comparison results of the simulation and experiment to verify the feasibility of the control scheme. Finally, Section V concludes this article.

II. Problem Description and Assumption

A. Mathematical Model of SPMSM

The dynamic equations of an SPMSM in the *dq* rotating frame can be expressed as follows:

$$\dot{\omega} = \frac{1}{J}\left(\frac{3}{2}n_p\psi_f i_q - B\omega - T_L\right) \tag{1}$$

$$\dot{i}_q = \frac{1}{L_s}(u_q - R_s i_q - n_p\omega L_s i_d - n_p\omega\psi_f) \tag{2}$$

$$\dot{i}_d = \frac{1}{L_s}(u_d - R_s i_d + n_p\omega L_s i_q) \tag{3}$$

where

i_d, i_q	d-axis and q-axis stator currents.
u_d, u_q	d-axis and q-axis stator voltages.
L_s	stator inductance.
ω	mechanical rotor speed.
J	rotor moment of inertia.
B	viscous friction coefficient.
ψ_f	magnet flux linkage.
T_L	load torque.
n_p	number of pole pairs.
R_s	stator resistance.

The control objective of this system is to design the control inputs to ensure that the dynamic performance of the system is not affected by parameter mismatch. The proposed controller is based on the following two assumptions.

Assumption 1: The dynamic response of the current loop is much faster than the rotor speed loop, i.e., they satisfy the two-time-scale separation principle.

Assumption 2: The motor parasitic parameters of viscous friction coefficient B, rotor moment of inertia J, stator resistance R_s, and magnet flux linkage ψ_f are considered to be unknown and vary slowly during a short sampling time. Besides, the load torque T_L is unknown and slowly varies in a short sampling period.

B. Conventional MRAC Revisit

Based on Assumption 1, (1) can be rewritten as follows:

$$\dot{\omega} = -a\omega + bi_q^* - d \tag{4}$$

where i_q^* is the q-axis current reference, which can be regarded as a control input for (4), and $a := B/J$, $d := T_L/J$, and $b := 1.5n_p\psi_f/J$.

The speed tracking error is defined as follows:

$$e_\omega = \omega - \omega^* \tag{5}$$

where ω^* is the speed reference.

According to (4) and (5), the speed-tracking error dynamic equations can be derived as follows:

$$\dot{e}_\omega = -ae_\omega + bi_q^* - a\omega^* - d. \tag{6}$$

The reference model of the conventional MRAC proposed in [26] is chosen as follows:

$$\dot{\omega}_m + \lambda_m\omega_m = 0 \tag{7}$$

where ω_m is the output of the reference model and $\lambda_m > 0$.

The reference model tracking error can be defined as $\sigma \triangleq \omega_m - e_\omega$. The dynamic equations of σ can be derived as follows:

$$\begin{aligned}\dot{\sigma} &= -\lambda_m\omega_m + a\omega - bi_q^* + d \\ &= -b\left(i_q^* + \boldsymbol{\delta}\boldsymbol{\xi}^T\right)\end{aligned} \tag{8}$$

where $\boldsymbol{\delta} = [a/b \quad \lambda_m/b \quad d/b]$ and $\boldsymbol{\xi}^T = [-\omega \quad \omega_m \quad -1]$.

The speed controller can be designed as follows:

$$i_q^* = \kappa\sigma - \hat{\boldsymbol{\delta}}\boldsymbol{\xi}^T \tag{9}$$

where $\kappa > 0$ is the gain of the controller, and $\hat{\boldsymbol{\delta}}$ denote the adaptive terms of $\boldsymbol{\delta}$.

Substituting (9) into (8) to get the following:

$$\dot{\sigma} = -\kappa b\sigma - b\tilde{\boldsymbol{\delta}}\boldsymbol{\xi}^T \tag{10}$$

where $\tilde{\boldsymbol{\delta}} = \boldsymbol{\delta} - \hat{\boldsymbol{\delta}}$ is the estimation error of the adaptive terms.

According to (10), the reference model tracking error dynamic can be expressed as follows:

$$\sigma = -\frac{b}{s + \kappa b}\left(\tilde{\boldsymbol{\delta}}\boldsymbol{\xi}^T\right). \tag{11}$$

It can be concluded from (11) that the closed-loop pole of the reference model tracking error system will be closer to

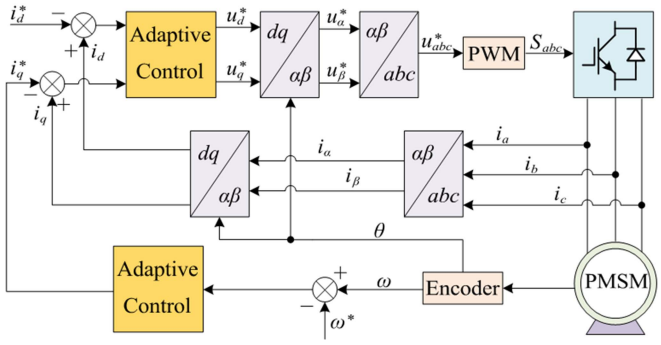

Fig. 1. Overall control block diagram of the proposed controller.

the imaginary axis as the moment of inertia increases. This means the dynamic response of the system will deteriorate, and the overshoot will increase. In addition, when the moment of inertia is reduced, the pole of the transfer function (11) will be farther away from the imaginary axis, which means the dynamic performance of the system will be improved. However, since most PMSM controllers are cascaded control structures that satisfy the two-time-scale separation principle, the bandwidth of the speed controller should be much smaller than the current controller bandwidth. Excessive speed loop bandwidth poses a potential risk to system stability.

III. Controller Design and Stability Analysis

To address the abovementioned problems, a cascaded adaptive controller characterized by parameter estimation convergence is designed in this section. The overall control block diagram of the proposed controller is presented in Fig. 1.

A. Adaptive Current Controller Based on I&I Methodology

By selecting i_d and i_q as the state variable x_1 and x_2, respectively. The equivalent form of (2) and (3) can be written as follows:

$$\dot{\boldsymbol{x}} = \frac{1}{L_s}\boldsymbol{u_i} + \boldsymbol{\delta}(\boldsymbol{x}) - \frac{1}{L_s}\boldsymbol{\phi}(\boldsymbol{x})\boldsymbol{\eta} \tag{12}$$

where $\boldsymbol{x} := \begin{bmatrix} i_d \\ i_q \end{bmatrix}$, $\boldsymbol{u_i} := \begin{bmatrix} u_d \\ u_q \end{bmatrix}$, $\boldsymbol{\delta}(\boldsymbol{x}) := \begin{bmatrix} n_p\omega i_q \\ -n_p\omega i_d \end{bmatrix}$, $\boldsymbol{\phi}(\boldsymbol{x}) := \begin{bmatrix} i_d & 0 \\ i_q & n_p\omega \end{bmatrix}$, and $\boldsymbol{\eta} := \begin{bmatrix} R_s \\ \psi_f \end{bmatrix}$.

In order to facilitate the controller design, model (4) is converted into the error model, turning the tracking problem into the regulation problem. The current tracking error vector $\mathbf{e}_i^T = [e_{id} \quad e_{iq}]$ is defined as follows:

$$\begin{bmatrix} e_{id} \\ e_{iq} \end{bmatrix} = \begin{bmatrix} i_d - i_d^* \\ i_q - i_q^* \end{bmatrix} \tag{13}$$

where i_d^* and i_q^* denote the reference values of the d-axis current and q-axis current, respectively.

According to (12) and (13), the current tracking error dynamic equation can be derived as follows:

$$\dot{\boldsymbol{e}}_{\boldsymbol{i}} = \frac{1}{L_s}\boldsymbol{u_i} + \boldsymbol{\delta}(\boldsymbol{x}) - \frac{1}{L_s}\boldsymbol{\phi}(\boldsymbol{x})\boldsymbol{\eta}. \tag{14}$$

Proposition 1: Consider the system (14), according to the certainty equivalence approach of adaptive control [31], the control law can be designed as follows:

$$\boldsymbol{u_i} = -\mathbf{K_{ic}}\boldsymbol{e_i} - L_s\boldsymbol{\delta}(\boldsymbol{x}) + \boldsymbol{\phi}(\boldsymbol{x})\hat{\boldsymbol{\eta}} \tag{15}$$

where $\mathbf{K_{ic}}$=diag$[k_d, k_q]$ is the controller gain matrix to be designed, and $\hat{\boldsymbol{\eta}}$ is the adaptive term, which denotes the estimate of R_s and ψ_f.

According to the I&I methodology described in [32], the update law of $\hat{\boldsymbol{\eta}}$ can be designed as follows:

$$\begin{cases} \hat{\boldsymbol{\eta}} = -\boldsymbol{\gamma}\boldsymbol{\xi} - \boldsymbol{\lambda}\boldsymbol{\beta}(\boldsymbol{x}) \\ \dot{\boldsymbol{\xi}} = \frac{\boldsymbol{\lambda}}{\boldsymbol{\gamma}L_s}\left(\nabla_{\boldsymbol{x}}\boldsymbol{\beta}\right)\mathbf{K}_{ic}\boldsymbol{e_i} \\ \boldsymbol{\beta} = \begin{bmatrix} \frac{1}{2}i_d^2 + \frac{1}{2}i_q^2 \\ n_p\omega i_q \end{bmatrix} \end{cases} \tag{16}$$

where $\boldsymbol{\gamma}$=diag$[\gamma_1, \gamma_2] > 0$, $\boldsymbol{\lambda}$=diag$[\lambda_1, \lambda_2] > 0$ are the adaptive gains matrices, and $\nabla_{\boldsymbol{x}}\boldsymbol{\beta} = \partial\boldsymbol{\beta}/\partial\boldsymbol{x}$.

Then, the current tracking error vector $\boldsymbol{e_i}$ will converge to zero as $t \to \infty$. Besides, the estimation error $\tilde{\boldsymbol{\eta}} = \boldsymbol{\eta} - \hat{\boldsymbol{\eta}}$ of the adaptive term has asymptotically stable equilibrium points at the origin.

Proof: According to the Assumption 2, the following function can be derived from (16):

$$\begin{aligned} \dot{\tilde{\boldsymbol{\eta}}} &= \boldsymbol{\gamma}\dot{\boldsymbol{\xi}} + \boldsymbol{\lambda}\frac{\partial\boldsymbol{\beta}(\boldsymbol{x})}{\partial\boldsymbol{x}}\dot{\boldsymbol{x}} \\ &= \boldsymbol{\lambda}\boldsymbol{\phi}^T(\boldsymbol{x})\mathbf{K}_{ic}\boldsymbol{e_i} + \boldsymbol{\lambda}\boldsymbol{\phi}^T(\boldsymbol{x})\dot{\boldsymbol{x}}. \end{aligned} \tag{17}$$

Taking (15) into (12) and (14), the current model and the current error model can be derived as follows:

$$\dot{\boldsymbol{x}} = \mathbf{A}_c\boldsymbol{e_i} - \frac{1}{L_s}\boldsymbol{\phi}(\boldsymbol{x})\tilde{\boldsymbol{\eta}} \tag{18}$$

$$\dot{\boldsymbol{e}}_{\boldsymbol{i}} = \mathbf{A}_c\boldsymbol{e_i} - \frac{1}{L_s}\boldsymbol{\phi}(\boldsymbol{x})\tilde{\boldsymbol{\eta}} \tag{19}$$

where $\mathbf{A}_c = \text{diag}[-\frac{k_d}{L_s}, -\frac{k_q}{L_s}]$ is a Hurwitz matrix.

According to (19), a candidate Lyapunov function is constructed as follows:

$$V_1 = \frac{1}{2}\boldsymbol{e_i}^T\boldsymbol{e_i} + \frac{1}{2}\tilde{\boldsymbol{\eta}}^T\boldsymbol{\lambda}^{-1}\tilde{\boldsymbol{\eta}}. \tag{20}$$

Taking the derivative of (20) with respect to time along the trajectory of (19) yields the following:

$$\dot{V}_1 = \boldsymbol{e_i}^T\mathbf{A}_c\boldsymbol{e_i} - \frac{\boldsymbol{e_i}^T\boldsymbol{\phi}\tilde{\boldsymbol{\eta}}}{2L_s} - \frac{\tilde{\boldsymbol{\eta}}^T\boldsymbol{\phi}^T\boldsymbol{e_i}}{2L_s} + \tilde{\boldsymbol{\eta}}^T\boldsymbol{\lambda}^{-1}\dot{\tilde{\boldsymbol{\eta}}}. \tag{21}$$

Substituting (17) and (18) into (21) to obtain the following:

$$\begin{aligned} \dot{V}_1 &\leqslant \lambda_{\max}(\mathbf{A}_c)\left|\boldsymbol{e_i}\right|^2 - \frac{\boldsymbol{e_i}^T\boldsymbol{\phi}\tilde{\boldsymbol{\eta}}}{2L_s} - \frac{\tilde{\boldsymbol{\eta}}^T\boldsymbol{\phi}^T\boldsymbol{e_i}}{2L_s} - \frac{1}{L_s}\tilde{\boldsymbol{\eta}}^T\boldsymbol{\phi}^T\boldsymbol{\phi}\tilde{\boldsymbol{\eta}} \\ &\leqslant \lambda_{\max}(\mathbf{A}_c)\left|\boldsymbol{e_i}\right|^2 + \frac{1}{2L_s}\left|\boldsymbol{e_i}\right|^2 + \frac{1}{2L_s}\left|\boldsymbol{\phi}\tilde{\boldsymbol{\eta}}\right|^2 - \frac{1}{L_s}\left|\boldsymbol{\phi}\tilde{\boldsymbol{\eta}}\right|^2 \end{aligned}$$

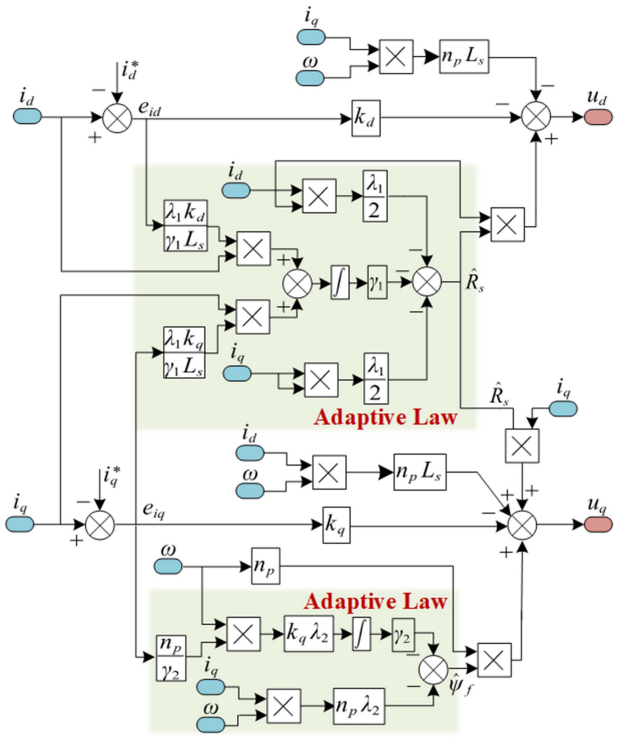

Fig. 2. Control block diagram of the current controller.

$$\leqslant \left(\lambda_{\max}(\mathbf{A}_c) + \frac{1}{2L_s}\right)|\boldsymbol{e_i}|^2 - \frac{1}{2L_s}|\boldsymbol{\phi}\tilde{\boldsymbol{\eta}}|^2. \tag{22}$$

According to (22), $\dot{V}_1$ is negative definite as long as $\lambda_{\max}(\mathbf{A}_c) < -1/(2L_s)$ and $\boldsymbol{\phi}^T(\boldsymbol{x})\boldsymbol{\phi}(\boldsymbol{x}) > 0$. Specifically, the current loop controller gain should meet $k_d > 0.5$ and $k_q > 0.5$. In addition, the speeds ω and i_d cannot be equal to zero. Using the Lyapunov's stability theorem, it can be concluded that $\lim_{t\to\infty}|e_{iq}(t)| = 0$ and $\lim_{t\to\infty}|\tilde{\boldsymbol{\eta}}| = 0$. □

To summarize, Fig. 2 shows the control block diagram of the current controller.

B. MRAC Speed Controller Design

To ensure that the closed-loop poles of the designed speed controller do not change with the parameter drift. The reference model of (6) can be designed as follows:

$$\dot{x}_m = -a_m x_m + r \tag{23}$$

where $a_m > 0$ and $r(t)$ is the input of the reference model. a_m and $r(t)$ are chosen such that x_m represents the desired state response of (6).

The reference model tracking error can be defined as $e_m \triangleq x_m - e_\omega$. Then, the following error dynamic model can be derived from (6) and (23):

$$\begin{aligned}\dot{e}_m &= \dot{x}_m - \dot{e}_\omega \\ &= -a_m e_m - b\left(i_q^* - ke_\omega - lr - q\right)\end{aligned} \tag{24}$$

where $k := (a - a_m)/b$, $l := 1/b$, and $q := (a\omega^* + d)/b$.

Proposition 2: To ensure that e_ω can track x_m for any reference model input signal $r(t)$, the control law can be chosen as follows:

$$i_q^* = \hat{k}e_\omega + \hat{l}r + \hat{q} \tag{25}$$

where $\hat{k}$, $\hat{l}$, and $\hat{q}$ denote the estimates of k, l, and q, respectively. The adaptive update laws of $\hat{k}$, $\hat{l}$, and $\hat{q}$ are given as follows:

$$\begin{cases}\dot{\hat{k}} = \gamma_3 e_m e_\omega \\ \dot{\hat{l}} = \gamma_4 r e_m \\ \dot{\hat{q}} = \gamma_5 e_m\end{cases} \tag{26}$$

where $\gamma_3 > 0$, $\gamma_4 > 0$, and $\gamma_5 > 0$ are the adaptive gains for $\hat{k}$, $\hat{l}$, and $\hat{q}$, respectively.

Then, the reference model tracking error e_m will converge to zero as $t \to \infty$.

Proof: The estimation error of adaptive terms can be defined as follows:

$$\begin{cases}\tilde{k} = k - \hat{k} \\ \tilde{l} = l - \hat{l} \\ \tilde{q} = q - \hat{q}.\end{cases} \tag{27}$$

Based on the Assumption 2, the following function can be derived from (26) and (27):

$$\begin{cases}\dot{\tilde{k}} = \dot{k} - \dot{\hat{k}} = -\gamma_3 e_m e_\omega \\ \dot{\tilde{l}} = \dot{l} - \dot{\hat{l}} = -\gamma_4 r e_m \\ \dot{\tilde{q}} = \dot{q} - \dot{\hat{q}} = -\gamma_5 e_m.\end{cases} \tag{28}$$

Taking (25) into (24), the error model is derived as follows:

$$\dot{e}_m = -a_m e_m + b\tilde{k}e_\omega + b\tilde{l}r + b\tilde{q}. \tag{29}$$

To verify the stability of the error model (29), a Lyapunov function is constructed as follows:

$$V_2 = \frac{1}{2}e_m^2 + \frac{b}{2\gamma_3}\tilde{k}^2 + \frac{b}{2\gamma_4}\tilde{l}^2 + \frac{b}{2\gamma_5}\tilde{q}^2. \tag{30}$$

Taking the derivative of (30) with respect to time along the trajectory of (29) yields the following:

$$\begin{aligned}\dot{V}_2 = &-a_m e_m^2 + b\tilde{k}e_\omega e_m + b\tilde{l}re_m + b\tilde{q}e_m \\ &+ \frac{b}{\gamma_3}\tilde{k}\dot{\tilde{k}} + \frac{b}{\gamma_4}\tilde{l}\dot{\tilde{l}} + \frac{b}{\gamma_5}\tilde{q}\dot{\tilde{q}}.\end{aligned} \tag{31}$$

Substitute (28) into (31) to get the following:

$$\dot{V}_2 = -a_m e_m^2 \leq 0. \tag{32}$$

Equations (30) and (32) only guarantee $e_m \in L_\infty$, but the convergence cannot be guaranteed (i.e., $e_m \notin L_2$). Integrating both sides of (32) gives

$$\int_0^\infty |e_m(t)|^2 dt \leqslant \frac{V_2(0) - V_2(\infty)}{a_m}. \tag{33}$$

Since $V_2(t) \geq 0$ and $\dot{V}_2(t) \leq 0$, the following inequality can be derived:

$$\int_0^\infty |e_m(t)|^2 dt \leq \infty \tag{34}$$

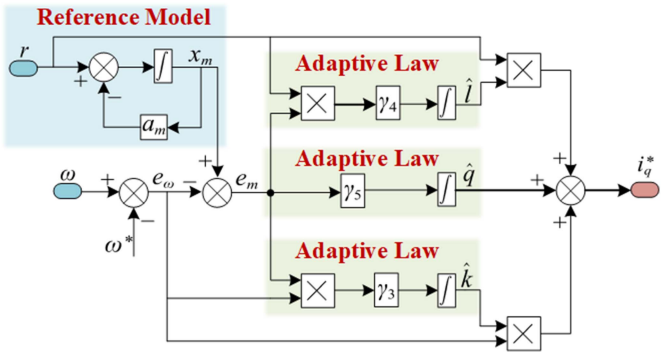

Fig. 3. Control block diagram of the speed controller.

which means the left-hand side of (34) is bounded. Using Barbalat's lemma [33], it can be concluded that $\lim_{t\to\infty}|e_m(t)|=0$. ■

The control block diagram of the speed controller based on MRAC is shown in Fig. 3.

C. Persistent Excitation Condition

The PE condition is indispensable to ensure the precise estimation of adaptive terms. This section will investigate the existence of PE in the proposed adaptive laws.

After adding and subtracting $-a_m e_\omega + r$, the speed tracking error model (6) can be rewritten as follows:

$$\dot{e}_\omega = -a_m e_\omega + r + b\left(i_q^* - k e_\omega - l r - q\right). \tag{35}$$

Substitute (25) into (35) to get the following:

$$\dot{e}_\omega = -\left(a_m + b\tilde{k}\right)e_\omega + \left(1 - b\tilde{l}\right)r - b\tilde{q}. \tag{36}$$

The speed tracking error dynamic of (36) can be expressed as follows:

$$e_\omega = \underbrace{\frac{1-b\tilde{l}}{s+\left(a_m+b\tilde{k}\right)}}_{H_1(s)} r - \underbrace{\frac{b}{s+\left(a_m+b\tilde{k}\right)}}_{H_2(s)}\tilde{q} \tag{37}$$

where s is the differential operator.

Proposition 3: The reference model input signal $r(t)$ can be selected as follows:

$$r(t) = A_1 \sin(\omega_1 t) \tag{38}$$

where $A_1 > 0$ and $\omega_1 > 0$.

Then, the adaptive update laws designed in (26) can guarantee that $\hat{k}(t)\to k$, $\hat{l}(t)\to l$, and $\hat{q}\to q$ exponentially fast, which means the poles of the transfer function $H_1(s)$ and $H_2(s)$ in (37) do not change with the parasitic parameters a, b, and d mismatch.

Proof: According to (25), the parameter vector to be estimated can be defined as $\hat{\boldsymbol{\theta}} = (\hat{k} \quad \hat{l} \quad \hat{q})^T$, and the regression vector is defined as $\boldsymbol{\Psi} = (e_\omega \quad r \quad 1)^T$. Then, (25) can be rewritten as follows:

$$i_q^* = \hat{\boldsymbol{\theta}}^T \boldsymbol{\Psi}. \tag{39}$$

Substitute (38) into (37), the expression of e_ω in the steady state can be derived as follows:

$$e_\omega(t) = A_2 \sin(\omega_1 t + \varphi) + B \tag{40}$$

where A_2 and φ are the amplitude and phase of the trigonometric function obtained by $r(t)$ after passing the transfer function $H_1(s)$, respectively, and $B \in L_\infty$ is obtained by $\tilde{q}$ after passing the transfer function $H_2(s)$.

The expression of $\boldsymbol{\Psi}(t)\boldsymbol{\Psi}^T(t)$ can be written as follows:

$$\boldsymbol{\Psi}(t)\boldsymbol{\Psi}^T(t) = \begin{pmatrix} e_\omega^2 & e_\omega r & e_\omega \\ r e_\omega & r^2 & r \\ e_\omega & r & 1 \end{pmatrix}. \tag{41}$$

Suppose that $T = 2\pi/\omega_1$. Substituting (38) and (40) into (41) and integrating it to get the following:

$$\int_t^{t+T} \boldsymbol{\Psi}(\tau)\boldsymbol{\Psi}^T(\tau)\,d\tau = \frac{2\pi}{\omega_1}\begin{pmatrix} \frac{A_2^2}{2}+B^2 & \frac{A_1A_2}{2}\cos\varphi & B \\ \frac{A_1A_2}{2}\cos\varphi & \frac{A_1^2}{2} & 0 \\ B & 0 & 1 \end{pmatrix}. \tag{42}$$

It can be observed that the leading principal minors of the symmetric matrix (42) are all greater than zero, which implies that (42) is a positive definite matrix. Therefore, there must exist a constant $\alpha_0 > 0$ satisfying the following condition [34]:

$$\int_t^{t+T} \boldsymbol{\Psi}(\tau)\boldsymbol{\Psi}^T(\tau)d\tau \geq \alpha_0 \boldsymbol{I}_{3\times 3} \quad \forall t \geq 0. \tag{43}$$

Based on the above discussions, it can be concluded that the updating laws designed in (26) satisfy the condition of PE, which means the parameter vector to be estimated $\hat{\boldsymbol{\theta}}(t)$ can exponentially converge to the true values. □

D. Controller Design

According to the above discussions, the parameters to be designed for the proposed controller include $\mathbf{K_{ic}}$, a_m, $r(t)$, λ_n, and γ_n. The specific design steps and parameter selection methods of the controller are summarized as follows.

Step 1: Select a suitable controller gain matrix $\mathbf{K}_{ic}$ in (15) to guarantee that $\mathbf{A}_c$ in the current tracking error dynamic equation (19) is a Hurwitz matrix.

The bandwidth of the current controller is recommended to be less than 1/10 of the switching frequency [24]. In addition, to guarantee the negative definiteness of $\dot{V}_1$ in (22), the matrix $\mathbf{A}_c$ should meet $\lambda_{\max}(\mathbf{A}_c) < -1/(2L_s)$. Combined with the current error model in (19), the value of the gain matrix $\mathbf{K_{ic}}$ can be obtained.

Step 2: Choose a positive a_m to ensure that the reference model (23) of the speed tracking error system (6) is stable.

To guarantee the rationality of Assumption 1 in Section II, the bandwidth of the speed controller should be much smaller than the current controller bandwidth. Once the bandwidth of the speed controller is determined, the values of a_m can be determined.

Step 3: Designed an appropriate input $r(t)$ of the reference model to ensure that the steady-state value of e_ω in (40) satisfies the PE condition in (43).

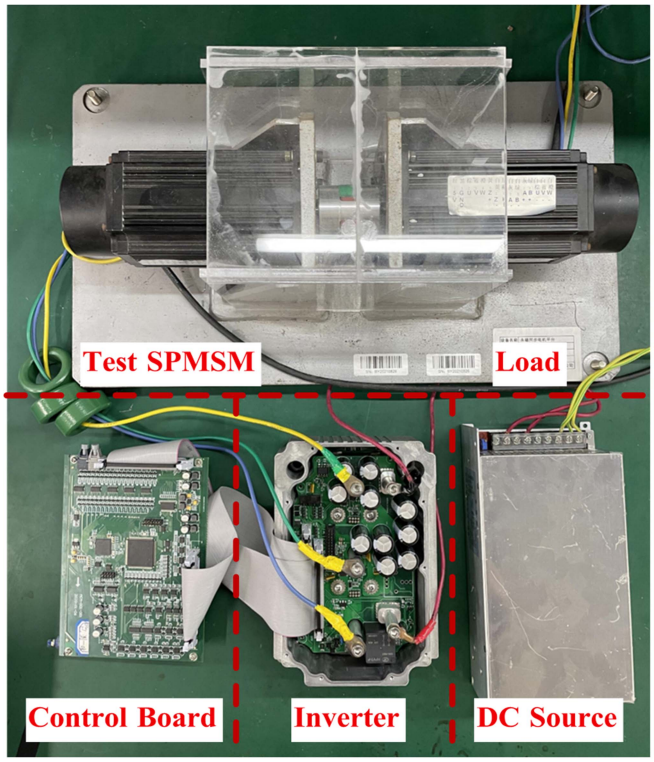

Fig. 4. Prototype of the laboratory platform.

Step 4: Choose the positive adaptive gains γ_n and λ_n to guarantee that the Lyapunov function of the system is positive definite.

Due to the presence of unmodeled dynamics in practical systems, γ_n and λ_n cannot be too large to avoid instability. Suitable adaptive gains are selected by trial and error [20].

IV. Simulation and Experimental Results

In this section, the effectiveness of the proposed control scheme is verified by some simulations in Simulink of Matlab2021b and the experiments on a prototype SPMSM drive with a TI TMS320F28335 DSP, which is shown in Fig. 4. In the experiment, the load torque step is realized by switching the load resistance of the load motor. To evaluate the performance of the proposed method, the MRAC proposed in [26] and the conventional PI controller are applied in the speed regulation loop for comparison. For a fair comparison, the nominal closed-loop poles of different controllers should be identical, and the current loop of the three controllers all use the proposed adaptive control scheme. The d-axis current reference (i_d^*) can be set as -1, to guarantee the negative definiteness of $\dot{V}_1$ in (22). In this way, parameter estimation errors of R_s and ψ_f are asymptotically stable. The parameters of the SPMSM are listed in Table I.

The controller in [26] is designed as follows:

$$i_q^* = \kappa\chi - \hat{\zeta}_1\omega - \hat{\zeta}_2\omega_m - \hat{\zeta}_3 \tag{44}$$

TABLE I
Parameters of the Experimental Setup

Symbol	Description	Value
J	Moment of inertia	0.0015 [kg·m^2]
B	Viscous friction coefficient	0.0002 [N·m·s/rad]
ψ_f	Rotor flux linkage	0.007235 [Wb]
n_p	Number of pole pairs	5
L_s	Stator inductances	0.1 [mH]
R_s	Stator resistance	0.017 [Ω]
ω^*	Speed reference	1000 [r/min]
V_{dc}	DC-link voltage	24 [V]
f_s	Switching frequency	10 [kHz]
ω_{rated}	Rated speed	3000 [r/min]

where $\kappa > 0$ is the gain of the controller, $\chi := \lambda e_{\omega 2} + e_\omega$, $e_{\omega 2} := \int e_\omega dt$, and $\hat{\zeta}_1, \hat{\zeta}_2$, and $\hat{\zeta}_3$ are the adaptive terms designed in [26].

The conventional PI controller is designed as follows:

$$i_q^* = K_p e_\omega + K_i \int_0^t e_\omega d\tau \tag{45}$$

where K_p and K_i are the gains of the PI controller.

For a fair comparison, the poles of the speed closed-loop system using the three controllers are identical, and the current loop of the three controllers all use the proposed adaptive control scheme.

A. Simulation Results

In order to evaluate the robustness and dynamic response of the three controllers under the parameter mismatch, the simulations were carried out under the following two cases.

1) *Case I:* Variation of moment of inertia J_n
2) *Case II:* Variation of load torque T_L .

Fig. 5 shows the simulation results of the speed response using three controllers under different moments of inertia. It can be concluded from the results that as the moment of inertia increases, the dynamic performance of the system both deteriorates under the MRAC proposed in [26] and the conventional PI controller. Specifically, the speed overshoot under the MRAC proposed in [26] and the conventional PI controller increased by 6 and 8 r/min, respectively. In contrast, when the moment of inertia is increased, the speed overshoot remains almost unchanged under the proposed control scheme. In addition, when the moment of inertia is reduced, the dynamic response of the motors under the MRAC proposed in [26] and the conventional PI controller are both improved. However, since the bandwidth of the speed controller should be much smaller than the current controller bandwidth, excessive speed loop bandwidth poses a potential risk to system stability. In contrast, the dynamic response of the motors does not increase as the moment of inertia reduces under the proposed control scheme. The abovementioned analysis results indicate that different from the two control schemes compared, the dynamic performance of the system is hardly affected by the moment of inertia drift under the proposed control scheme. This verifies the correctness of Proposition 3.

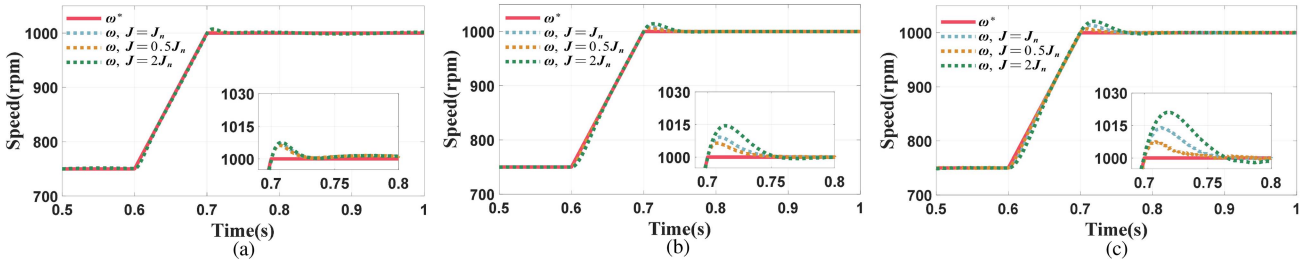

Fig. 5. Simulation results of three control schemes under different moment of inertia. (a) Proposed scheme. (b) MRAC in [26]. (c) Conventional PI controller.

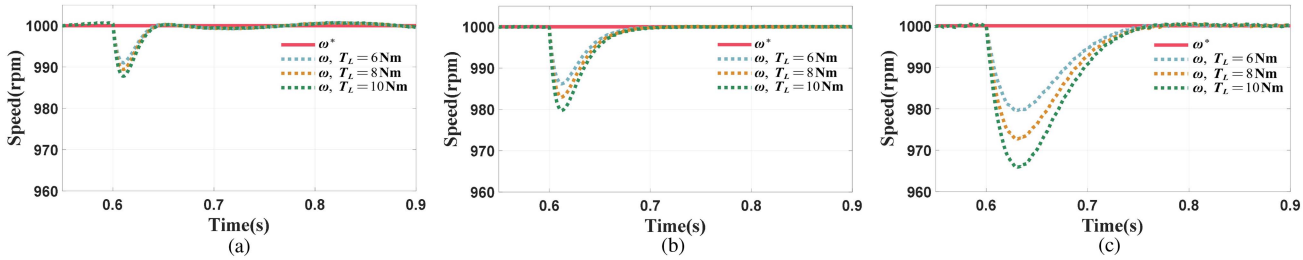

Fig. 6. Simulation results of three control schemes under the load torque step. (a) Proposed scheme. (b) MRAC in [26]. (c) Conventional PI controller.

Fig. 6 illustrates the responses of speed under the load torque step by using different controllers. Although all three control strategies are able to regulate the speed return to their reference values under the load torque step, the speed drop under the proposed controller and the control scheme proposed in [26] are smaller than the conventional PI controller. This is because the two control schemes compensate for load disturbance through adaptive terms. Specifically, the proposed control scheme has the smallest speed drop with 13 r/min under three different load torques. When using the MRAC proposed in [26] and conventional PI controller, the maximum speed drop is 20 and 34 r/min, respectively. The abovementioned results indicated that the proposed control strategy has better robustness to load disturbances.

Fig. 7(a) shows the simulation result of demagnetization protection. From the result, it can be concluded that the estimated value of the rotor flux linkage can track the true value. When the rotor flux linkage is too low, the system can detect and enter a protected state. Fig. 7(b) shows the simulation result of overheating protection. Since the resistance value of the stator resistance increases with temperature, it is possible to provide over temperature protection for the system by estimating the stator resistance. As can be seen from the results, when the stator resistance becomes large, the system can accurately detect and shutdown the system for protection.

Based on the above discussion, it can be concluded that the proposed control scheme is insensitive to changes in model parameters and has suppression capability for external disturbances. The dynamic response of the proposed control scheme is better than other controllers under parameter mismatch. Besides, the estimated stator resistance and rotor flux linkage can provide monitoring and protection for the system.

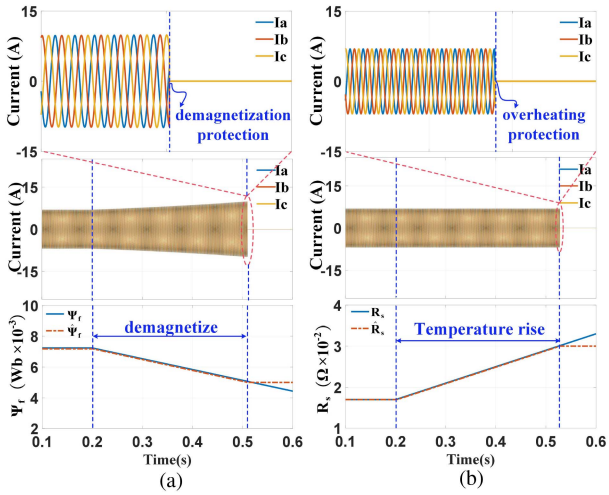

Fig. 7. Simulation results of system detection and protection. (a) Demagnetization protection. (b) Overheating protection.

B. Experimental Results

Fig. 8 shows the experimental result of the motor startup. From the result, it can be observed that all three control schemes can regulate the speed to the reference value. The proposed control scheme has a fast speed response with a settling time of 32 ms and an overshoot of 2.4%, the settling time of the MRAC proposed in [26] is 52 ms and the overshoot is 4.3%, and the conventional PI controller has a settling time of 112 ms and an overshoot of 7.3% . Based on the above discussion, it can be concluded that the proposed control scheme has a better dynamic response compared with the other two control schemes.

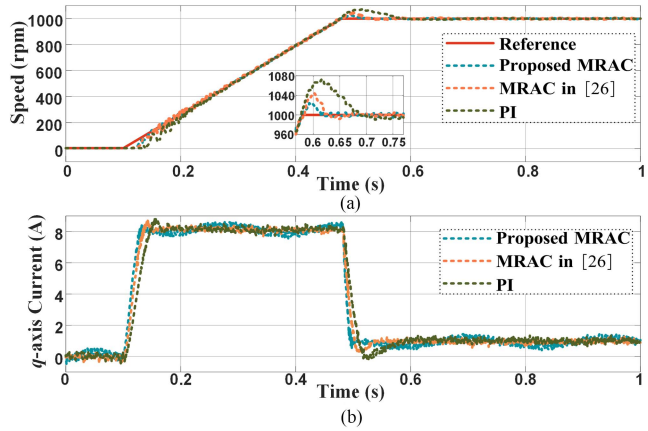

Fig. 8. Experimental result of the motor startup under three different control schemes. (a) Speed response. (b) q-axis currents.

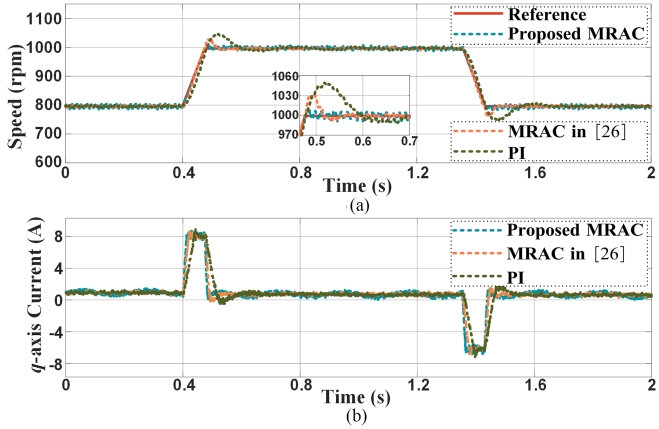

Fig. 9. Experimental result of the speed reference changes under three different control schemes. (a) Speed response. (b) q-axis currents.

Fig. 9 shows the experimental result of the three control schemes under the speed reference changes from 800 to 1000 r/min and back to 800 r/min. The result shows that all three control schemes can ensure that the speed can eventually track up the reference under the speed reference change. The MRAC proposed in [26] has an overshoot of 2.9%, and the settling time is 41 ms. With the conventional PI controller, the speed overshoot is 4.5% and the regulation time is 102 ms. In contrast, the proposed control scheme has the minimum overshoot and the shortest regulation time. The abovementioned results depict that the proposed control scheme exhibits better dynamic performance among the three controllers under the speed reference steps.

Fig. 10 illustrates the experimental result of the three control schemes at the load torque step. It can be observed that all control schemes are able to adjust the motor speed to the reference value after a sudden change in load torque. The speed response of the proposed control scheme shows the minimal speed drop with 30 r/min and the shortest settling time of 31 ms. When the speed loop uses the MRAC proposed in [26], the speed drop is 56 r/min and the settling time is 66 ms. Under the conventional PI control

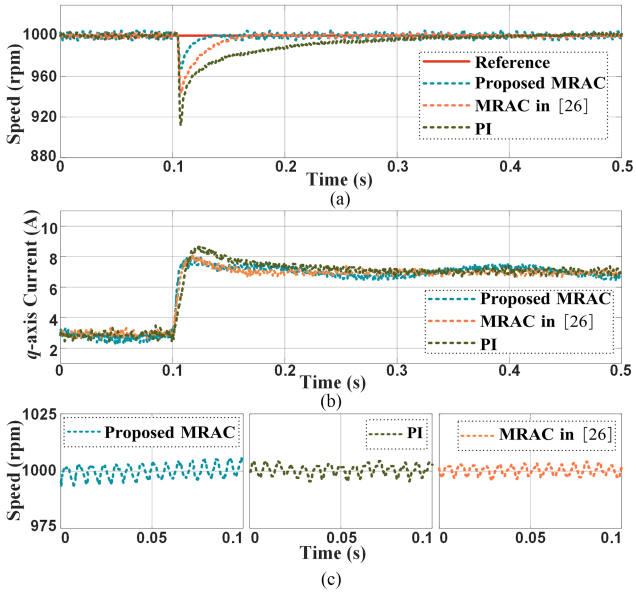

Fig. 10. Experimental result of the load torque step under three different control schemes. (a) Speed response. (b) q-axis currents. (c) Speed steady-state waveform.

scheme, the speed drop is 88 r/min, and the settling time is the longest among the three control schemes. The abovementioned results show that among the three control schemes, the proposed control scheme has stronger robustness to load torque changes and the fastest speed response recovery.

In addition, Fig. 10(c) presents the steady-state waveforms of the speed under three control schemes. The result shows that the maximum steady-state speed error under the proposed control scheme is 6 r/min. However, the maximum steady-state speed errors under the MRAC proposed in [26] and the conventional PI controller are 3 and 3.6 r/min, respectively. The reason for this phenomenon is that the reference model input signal $r(t)$ of the proposed control scheme is selected as the sinusoidal signal shown in (38), which results in the steady-state value of the speed tracking error is not zero. Although the nonzero reference model input signal increases the steady-state error of the system, the sinusoidal input signal can ensure that the adaptive terms estimation error is asymptotically stable. This character guarantees the desired dynamic performance of the system under parameter mismatch. Fig. 11 depicts the responses of the A-phase stator current when the load torque step.

Fig. 12 depicts the experimental results of speed reversal, in which the three control schemes are able to regulate the speed to its desired speed even under the speed reference is changed from 250 to -250 r/min. However, among the three control schemes, the conventional PI controller has the largest speed drop with 60 r/min and the longest settling time with 108 ms. Specifically, the speed drop of the MRAC proposed in [26] is 36 r/min and the settling time is 45 ms. Under the proposed control scheme, the speed drop is 19 r/min and the settling time is 24 ms. Based on the abovementioned analyses, it can be concluded that the proposed control scheme has better

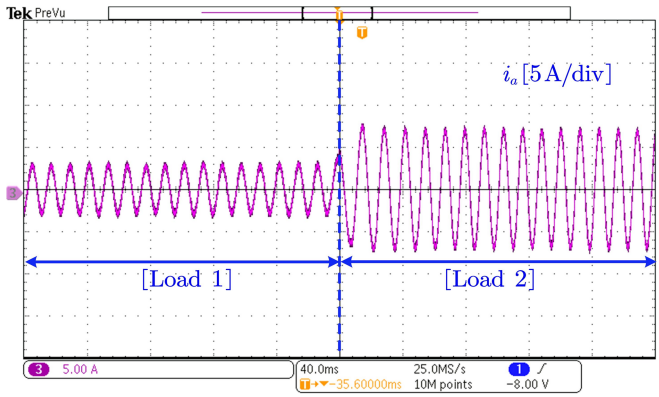

Fig. 11. Experimental result of the A-phase stator current under the load torque step.

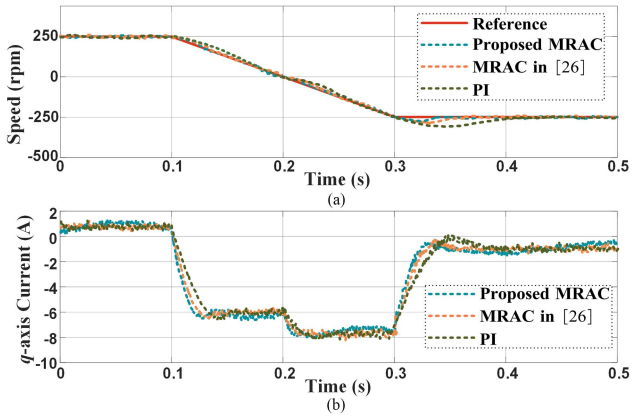

Fig. 12. Experimental result of speed reversal. (a) Speed response. (b) q-axis currents.

TABLE II
QUALITATIVELY COMPARISONS UNDER DIFFERENT CONTROLLERS

Comparative items		Motor startup	Speed command changes	Load torque step	Speed reversal
Maximum speed error (r/min)	(i)	24	9	30	19
	(ii)	43	29	56	36
	(iii)	73	45	88	60
Overshoot/ Undershoot (%)	(i)	2.4	0.9	3	1.9
	(ii)	4.3	2.9	5.6	3.6
	(iii)	7.3	4.5	8.8	6
Settling time (ms)	(i)	32	13	31	24
	(ii)	52	41	66	45
	(iii)	112	102	248	108

(i) Proposed Scheme. (ii) MRAC in [26]. (iii) Conventional PI controller.

dynamic performance among the three controllers under the speed reversal. The experimental comparison results of the three control schemes are summarized in Table II.

To verify the superiority of the proposed adaptive current controller, Fig. 13 shows the experimental results of the d-axis current step under different control strategies. It can be observed that both control schemes are able to regulate the current to their

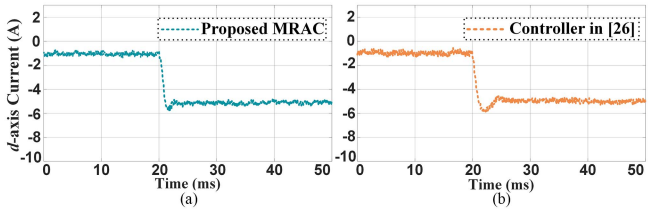

Fig. 13. Experimental results of d-axis current step using different controllers. (a) Proposed MRAC. (b) Controller in [26].

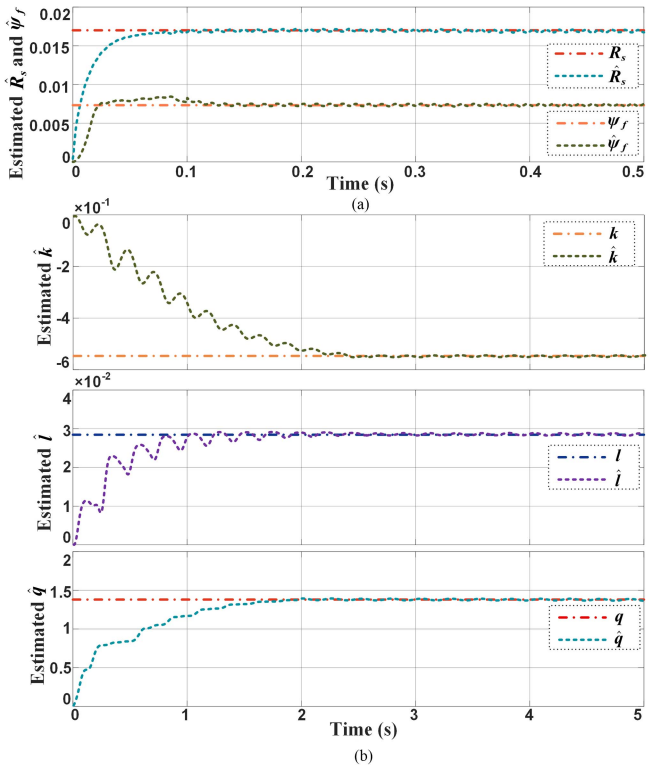

Fig. 14. Experimental estimation results of adaptive terms. (a) Adaptive terms in the current controller. (b) Adaptive terms in the speed controller.

references. However, the proposed adaptive current controller has a shorter settling time than the controller proposed in [26]. Specifically, the settling time of the controller proposed in [26] is 5.4 ms when the d-axis current step from -1 to -5A. In contrast, the settling time of the proposed adaptive current controller is only 2.6 ms. The results indicate that the proposed control strategy has better dynamic performance compared with the controller proposed in [26].

Fig. 14(a) and (b) depicts the estimation results of adaptive terms in the current controller and speed controller, respectively. The results show that all the adaptive terms can converge to the actual value eventually, which verifies the correctness of Propositions 1 and 3. The estimation of stator resistance and rotor flux linkage in the current loop can be used for providing detection and protection for the system, which improves the reliability of the system. The accurate estimation of the adaptive terms in the speed controller can ensure that the closed-loop

poles of the system do not change with parameter drift. This character guarantees the desired dynamic performance of the system under parameter mismatch.

V. Conclusion

In this article, a cascaded adaptive control scheme is proposed for SPMSM, which guarantees the robustness of the system against unknown parameters and external disturbances. The adaptive current controller is designed by following the immersion and invariance techniques to ensure the estimation error of the stator resistance and magnet flux linkage are globally convergent, which can be used for overheating protection and demagnetization protection. In addition, an MRAC-based speed controller is designed to guarantee the precise estimation of adaptive terms. It not only makes the system robust to SPMSM parameter uncertainties and external perturbations, but also guarantees the dynamic performance of the system under the parameter mismatch. The proposed control scheme, the MRAC proposed in [26], and the conventional PI controller are compared by simulations and experiments. The results show that the proposed control scheme among the three control schemes can achieve a faster dynamic response and stronger robustness under parameter uncertainties and external disturbances.

References

[1] X. Liu, H. Chen, J. Zhao, and A. Belahcen, "Research on the performances and parameters of interior PMSM used for electric vehicles," *IEEE Trans. Ind. Electron.*, vol. 63, no. 6, pp. 3533–3545, Jun. 2016.

[2] Y. A. R. I. Mohamed and E. F. El-Saadany, "A current control scheme with an adaptive internal model for torque ripple minimization and robust current regulation in PMSM drive systems," *IEEE Trans. Energy Convers.*, vol. 23, no. 1, pp. 92–100, Mar. 2008.

[3] J. Yang, W.-H. Chen, S. Li, L. Guo, and Y. Yan, "Disturbance/uncertainty estimation and attenuation techniques in PMSM drives—A survey," *IEEE Trans. Ind. Electron.*, vol. 64, no. 4, pp. 3273–3285, Apr. 2017.

[4] R. Errouissi, M. Ouhrouche, W.-H. Chen, and A. M. Trzynadlowski, "Robust cascaded nonlinear predictive control of a permanent magnet synchronous motor with antiwindup compensator," *IEEE Trans. Ind. Electron.*, vol. 59, no. 8, pp. 3078–3088, Aug. 2012.

[5] N. Maleki, M. R. A. Pahlavani, and I. Soltani, "A detailed comparison between FOC and DTC methods of a permanent magnet synchronous motor drive," *J. Elect. Electron. Eng.*, vol. 3, no. 2/1, pp. 92–100, 2015.

[6] M. Tursini, F. Parasiliti, and D. Zhang, "Real-time gain tuning of PI controllers for high-performance PMSM drives," *IEEE Trans. Ind. Appl.*, vol. 38, no. 4, pp. 1018–1026, Jul./Aug. 2002.

[7] X. Zhang, L. Sun, K. Zhao, and L. Sun, "Nonlinear speed control for PMSM system using sliding-mode control and disturbance compensation techniques," *IEEE Trans. Power Electron.*, vol. 28, no. 3, pp. 1358–1365, Mar. 2012.

[8] J. R. Dominguez, A. Navarrete, M. A. Meza, A. G. Loukianov, and J. Canedo, "Digital sliding-mode sensorless control for surface-mounted PMSM," *IEEE Trans. Ind. Informat.*, vol. 10, no. 1, pp. 137–151, Feb. 2014.

[9] M. L. Corradini, G. Ippoliti, S. Longhi, and G. Orlando, "A quasi-sliding mode approach for robust control and speed estimation of pm synchronous motors," *IEEE Trans. Ind. Electron.*, vol. 59, no. 2, pp. 1096–1104, Feb. 2012.

[10] Q. Hou, S. Ding, and X. Yu, "Composite super-twisting sliding mode control design for PMSM speed regulation problem based on a novel disturbance observer," *IEEE Trans. Energy Convers.*, vol. 36, no. 4, pp. 2591–2599, Dec. 2021.

[11] Y. Wang, Y. Feng, X. Zhang, and J. Liang, "A new reaching law for antidisturbance sliding-mode control of PMSM speed regulation system," *IEEE Trans. Power Electron.*, vol. 35, no. 4, pp. 4117–4126, Apr. 2020.

[12] S. Ding, Q. Hou, and H. Wang, "Disturbance-observer-based second-order sliding mode controller for speed control of PMSM drives," *IEEE Trans. Energy Convers.*, vol. 38, no. 1, pp. 100–110, Mar. 2023.

[13] F. Wang, L. He, and J. Rodríguez, "A robust predictive speed control for SPMSM systems using a sliding mode gradient descent disturbance observer," *IEEE Trans. Energy Convers.*, vol. 38, no. 1, pp. 540–549, Mar. 2023.

[14] M. Hu, W. Hua, Z. Wang, S. Li, P. Wang, and Y. Wang, "Selective periodic disturbance elimination using extended harmonic state observer for smooth speed control in PMSM drives," *IEEE Trans. Power Electron.*, vol. 37, no. 11, pp. 13288–13298, Nov. 2022.

[15] S. Li and H. Gu, "Fuzzy adaptive internal model control schemes for PMSM speed-regulation system," *IEEE Trans. Ind. Informat.*, vol. 8, no. 4, pp. 767–779, Nov. 2012.

[16] S. Barkat, A. Tlemçani, and H. Nouri, "Noninteracting adaptive control of PMSM using interval type-2 fuzzy logic systems," *IEEE Trans. Fuzzy Syst.*, vol. 19, no. 5, pp. 925–936, Oct. 2011.

[17] F.-J. Lin and C.-H. Lin, "A permanent-magnet synchronous motor servo drive using self-constructing fuzzy neural network controller," *IEEE Trans. Energy Convers.*, vol. 19, no. 1, pp. 66–72, Mar. 2004.

[18] H. Chaoui and P. Sicard, "Adaptive fuzzy logic control of permanent magnet synchronous machines with nonlinear friction," *IEEE Trans. Ind. Electron.*, vol. 59, no. 2, pp. 1123–1133, Feb. 2012.

[19] P. Mani, R. Rajan, L. Shanmugam, and Y. H. Joo, "Adaptive fractional fuzzy integral sliding mode control for PMSM model," *IEEE Trans. Fuzzy Syst.*, vol. 27, no. 8, pp. 1674–1686, Aug. 2019.

[20] Y. Yin et al., "Disturbance and uncertainty attenuation for speed regulation of PMSM servo system using adaptive optimal control strategy," *IEEE Trans. Transport. Electrific.*, vol. 9, no. 2, pp. 3410–3420, Jun. 2023.

[21] H. H. Choi, N. T.-T. Vu, and J.-W. Jung, "Digital implementation of an adaptive speed regulator for a PMSM," *IEEE Trans. Power Electron.*, vol. 26, no. 1, pp. 3–8, Jan. 2011.

[22] S. Li and Z. Liu, "Adaptive speed control for permanent-magnet synchronous motor system with variations of load inertia," *IEEE Trans. Ind. Electron.*, vol. 56, no. 8, pp. 3050–3059, Aug. 2009.

[23] J. Zhou and Y. Wang, "Real-time nonlinear adaptive backstepping speed control for a PM synchronous motor," *Control Eng. Pract.*, vol. 13, no. 10, pp. 1259–1269, 2005.

[24] S.-K. Kim, K.-G. Lee, and K.-B. Lee, "Singularity-free adaptive speed tracking control for uncertain permanent magnet synchronous motor," *IEEE Trans. Power Electron.*, vol. 31, no. 2, pp. 1692–1701, Feb. 2016.

[25] S.-K. Kim, J.-S. Lee, and K.-B. Lee, "Offset-free robust adaptive backstepping speed control for uncertain permanent magnet synchronous motor," *IEEE Trans. Power Electron.*, vol. 31, no. 10, pp. 7065–7076, Oct. 2016.

[26] A. T. Nguyen, M. S. Rafaq, H. H. Choi, and J.-W. Jung, "A model reference adaptive control based speed controller for a surface-mounted permanent magnet synchronous motor drive," *IEEE Trans. Ind. Electron.*, vol. 65, no. 12, pp. 9399–9409, Dec. 2018.

[27] A. R. Teja, C. Chakraborty, S. Maiti, and Y. Hori, "A new model reference adaptive controller for four quadrant vector controlled induction motor drives," *IEEE Trans. Ind. Electron.*, vol. 59, no. 10, pp. 3757–3767, Oct. 2012.

[28] H. Jin and J. Lee, "An RMRAC current regulator for permanent-magnet synchronous motor based on statistical model interpretation," *IEEE Trans. Ind. Electron.*, vol. 56, no. 1, pp. 169–177, Jan. 2009.

[29] L. Guo and L. Parsa, "Model reference adaptive control of five-phase IPM motors based on neural network," *IEEE Trans. Ind. Electron.*, vol. 59, no. 3, pp. 1500–1508, Mar. 2012.

[30] J. Li, Y. Sun, H. Dan, X. Li, F. Zhou, and M. Su, "Adaptive control for SPMSM no need of parameter information but pole pairs," *IEEE Trans. Power Electron.*, vol. 39, no. 3, pp. 3075–3085, Mar. 2024.

[31] P. A. Ioannou and J. Sun, *Robust Adaptive Control*. Upper Saddle River, NJ, USA: PTR Prentice-Hall, 1996.

[32] A. Astolfi and R. Ortega, "Immersion and invariance: A new tool for stabilization and adaptive control of nonlinear systems," *IEEE Trans. Autom. Control*, vol. 48, no. 4, pp. 590–606, Apr. 2003.

[33] J. Li, Y. Sun, X. Li, S. Xie, J. Lin, and M. Su, "Observer-based adaptive control for single-phase UPS inverter under nonlinear load," *IEEE Trans. Transport. Electrific.*, vol. 8, no. 2, pp. 2785–2796, Jun. 2022.

[34] R. Bitmead, "Persistence of excitation conditions and the convergence of adaptive schemes," *IEEE Trans. Inf. Theory*, vol. 30, no. 2, pp. 183–191, Mar. 1984.

Jiong Li was born in Hunan, China, in 1998. He received the B.S. degree in resource exploration engineering in 2020 from Central South University, Changsha, China, where he is currently working toward the Ph.D. degree in electrical engineering.

His current research interests include control of PMSM and stability analysis of power electronics devices.

Yao Sun (Member, IEEE) was born in Hunan, China, in 1981. He received the B.S. and M.S. degrees in automation, and the Ph.D. degree in control science and engineering from the School of Information Science and Engineering, Central South University, Changsha, China, in 2004, 2007, and 2010, respectively.

He has been a Professor with the School of Automation, Central South University. His research interests include matrix converter, microgrids, and wind energy conversion systems.

Hanbing Dan (Senior Member, IEEE) was born in Hubei, China, in 1991. He received the B.S. degree in automation and the Ph.D. degree in control science and engineering from Central South University, Changsha, China, in 2012 and 2017, respectively.

In 2017, he was a Visiting Researcher with the Faculty of Engineering, University of Nottingham, Nottingham, U.K. Since 2018, he has been with the School of Automation, Central South University where he is currently an Associate Professor. His research interests include power converter and motor control.

Xing Li was born in Hunan, China, in 1988. She received the B.S. degree in automation, and the Ph.D. degree in control science and engineering from the School of Information Science and Engineering, Central South University, Changsha, China, in 2009, and 2014, respectively.

She is currently an Associate Professor with the College of Electrical and Information Engineering, Hunan University, Changsha. Her research interests include power electronic converter and wind energy conversion system.

Feng Zhou (Member, IEEE) received the B.Eng., M.Eng., and Ph.D. degrees in control science and engineering from Central South University, Changsha, China, in 2009, 2012, and 2017, respectively.

He is currently an Associate Professor with the School of Electronic Information and Electrical Engineering, Changsha University. His main research focuses on high-performance predictive control technology for motor drive systems.

Mei Su (Member, IEEE) was born in Hunan, China, in 1967. She received the B.S. and M.S. degrees in automation and the Ph.D. degree in control theory and control engineering from the School of Information Science and Engineering, Central South University, Changsha, China, in 1989, 1992, and 2005, respectively.

She has been a Full Professor with the School of Automation, Central South University. Her research interests include matrix converter, adjustable speed drives, and wind energy conversion systems.

Dr. Su is currently an Associate Editor for IEEE TRANSACTIONS ON POWER ELECTRONICS and IEEE TRANSACTIONS ON SUSTAINABLE ENERGY.